GAUGE INVARIANCE STRUCTURE OF QUANTUM CHROMODYNAMICS

Predrag CVITANOVIĆ

Nordita, Blegdamsvej 17, DK-2100 Copenhagen Ø, Denmark

P.G. LAUWERS and P.N. SCHARBACH[1]

The Niels Bohr Institute, Copenhagen Ø, Denmark

Perturbative QCD may be subdivided into separately gauge-invariant sectors according to the projection of non-abelian color weights onto linearly independent basis elements. We exploit the general Lie group structure of the theory to give an algorithm for finding these gauge-invariant sets and present several examples of its use. The planar sector and the systematics of the non-planar corrections are defined for any gauge theory. Our gauge set classification has implications for QCD bound states, finite order perturbative QCD calculations, the study of QCD infrared singularities and for the question of convergence of the perturbation series.

1. Introduction

For the purposes of this paper we shall consider QCD as a non-abelian gauge theory of quarks and gluons defined by the perturbation expansion. The physics of the theory so defined may involve sums of infinite numbers of Feynman diagrams, but is perturbative in the sense that all contributions follow from the basic vertices of the theory, and not from non-perturbative phenomena such as instantons. At present we are unable to carry out the momentum integrations for arbitrarily complicated diagrams. On the other hand, one should investigate whether it is possible to organize this infinity of QCD diagrams before we tackle the problem of actually evaluating and summing them.

At first glance it would seem that there is not much that one can do. Each diagram is gauge dependent and physically meaningless by itself; the textbook proofs of gauge invariance of physical quantities assume the inclusion of all Feynman diagrams contributing in a given order. However, for quantum electrodynamics this is not the whole story; in actual perturbative calculations one soon discovers that the full set of diagrams may be subdivided into "gauge sets": subsets which are individually gauge invariant [1–3]. This decomposition can be very useful in practice, as it is often convenient to perform different parts of the calculation in different gauges [3]. It is

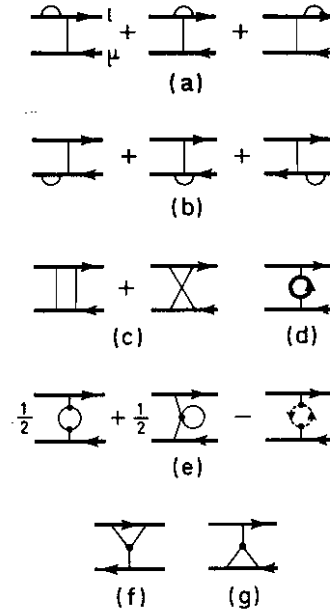[1] Present address: Rutherford Laboratory, Chilton, Didcot, Oxon., England.

Fig. 1. (a)–(d) order e^4 contributions to electron–muon scattering. (e)–(g) additional non-abelian diagrams for quark–quark scattering.

also important in the study of infrared (IR) singularities; IR singularities exponentiate grouped into sets of diagrams distinguished by the charged legs to which the photons are attached. After renormalization these sets are also separately gauge-invariant contributions to the S-matrix element [4–7].

This separation of QED diagrams into gauge-invariant subsets has a simple explanation; the Ward identities work separately for each charged line [8]. Consider for example the one-loop corrections to electron-muon scattering, fig. 1. Sets (a) and (b) are separately gauge invariant by the usual Ward-Takahashi identity which relates self-energy and vertex diagrams, and set (c) is gauge invariant as the photons are inserted in all symmetric ways.

The situation in non-abelian theories is less transparent: differing group-theoretic factors spoil the gauge invariance of sets (a), (b) and (c), and the new non-abelian diagrams (e), (f) and (g) now appear. The QCD Ward identities [9–11] do not work separately for each fermion line, and the QED concept of gauge-invariant subsets seems to be lost. Nevertheless, as we show in this paper, QCD gauge sets may be systematically identified. The key lies in exploiting the structure of the group theoretic color factors. The idea is somewhat analogous to the decomposition of scattering amplitudes for particles with spin into amplitudes of definite helicity; color is a kind of internal spin, and we can split up QCD amplitudes into different irreducible representations of the color "spin". Posed this way, the program would seem to require a formidable group-theoretic arsenal. Luckily, it turns out that the

less one assumes, the more powerful the results one obtains. We shall assume only that the quark-gluon couplings $(T_i)_b^a$ close a Lie algebra. That is the definition of a non-abelian gauge theory, and that is all we shall need to obtain the resolution of any gauge theory into a maximal number of gauge-invariant sectors. No particular gauge group or group representation is assumed.

The classification that emerges may be more than a convenient calculational aid. We show that every gauge theory has a gauge-invariant planar sector which coincides with 't Hooft's $N \rightarrow \infty$ limit of the $U(N)$ gauge theory [12–15].

The non-leading terms in the $1/N$ expansion, on the other hand, are decomposed into many gauge sets by the methods of this paper. We argue later that QED and QCD_2 provide examples of a dynamical ordering of gauge-invariant sectors in terms of the degree of infrared singularity. It remains to find an appropriate color basis for QCD in which the gauge sets are similarly ordered.

In sect. 2 we introduce a diagrammatic notation for group-theoretic color factors of QCD, and define the concept of color basis. In sect. 3 we associate a gauge set with each element of a color basis. Color bases for tree diagrams are constructed in sect. 4, and in sect. 5 we describe a systematic way of constructing color bases for diagrams with loops. In sect. 6 the relevance of gauge sets to the physics of QCD bound states is discussed. In sect. 7 we briefly examine the gauge sets for quark–quark scattering; this is of interest for the study of non-leading IR singularities in QCD. In sect. 7 we shall also give the gauge sets for the example just discussed, the diagrams of fig. 1. QED gauge sets are given in sect. 8. We summarize our results in sect. 9. Appendices A and B contain some additional group-theoretic results.

2. Color bases

In a non-abelian gauge theory the contribution of a Feynman diagram G to an amplitude is a product of three factors

$$A_G = W_G C_G F_G. \tag{2.1}$$

F_G is the momentum space factor, C_G is the combinatoric factor and W_G contains all the gauge group structure and will be referred to as the *color weight* of the diagram. Consider as an example diagram a of fig. 2. Its contribution to the QCD Compton scattering Green function is $W_a C_a F_a$, where

$$W_a = \delta_{ik}\delta_{jl}\delta_a^c (T_k)_c^d \delta_d^e (T_l)_e^f \delta_f^b, \tag{2.2}$$

$$C_a = 1, \tag{2.3}$$

$$F_a = \frac{-ig^{\mu\rho}}{k_1^2} \frac{-ig^{\nu\sigma}}{k_2^2} \frac{i}{\not{p}_2 - m} (-i\gamma_\mu)$$

$$\times \frac{i}{(\not{p}_2 + \not{k}_2 - \not{p}_1 - \not{k}_1) - m} (-i\gamma_\sigma) \frac{i}{\not{p}_1 - m}. \tag{2.4}$$
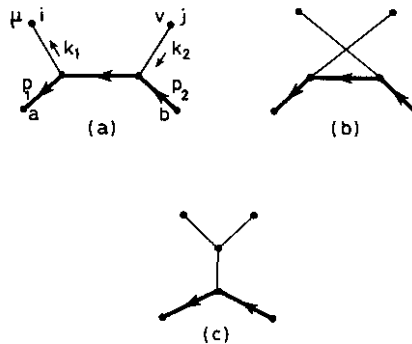
Fig. 2. Born term for Compton scattering in QCD.

We have chosen to write W_a as above, rather than as a product of group generators $(T_i)_c^a(T_j)_d^c$, to emphasize that the color weight itself can be thought of as a Feynman diagram.

In order to make the handling of color weights of more complicated diagrams easier and more transparent, we shall represent them diagrammatically [16]. The "propagators" and "vertices" for these color weight diagrams are defined in fig. 3a. Directed lines represent quarks in an N-dimensional representation of the gauge group of order d_A. Gluons are represented by thin undirected lines. Note that the four-gluon color vertex $c_{ijk}c_{lmk}$ is a product of three-gluon vertices. The three-gluon color vertex is an oriented vertex. Our convention for transcribing such a vertex as

Fig. 3. (a) Definitions of the propagators and vertices for color weight diagrams. (b) Lie algebra relation. (c) Invariance relation.

$-iC_{ijk}$ is that the indices should be read counterclockwise. The Lie algebra relation $[T_i, T_j] = iC_{ijk}T_k$ is represented graphically by fig. 3b. We shall use this relation to replace all structure constant factors C_{ijk} by products of T_i matrices. For color weights without C_{ijk} factors the Lie algebra amounts to the relation fig. 3c. This is a simple example of the invariance relations, described in appendix A, which we find very useful in the analysis of color weights.

The diagrammatic Lie algebra relation fig. 3b looks like a relation between Compton scattering diagrams, and indeed it is; it tells us that the color weights of the three Compton scattering diagrams (fig. 2) are not independent. For any non-abelian group only two of these three color weights are independent. For example, we can take W_a, W_b as independent weights, and eliminate W_c by the Lie algebra relation $W_a - W_b = W_c$.

This choice of independent color weights is the simplest example of a *color basis*. A color basis is a maximal set of color weights (in a given order of perturbation theory) which cannot be related by the Lie algebra relations. For a given color basis $T^{(1)}$, $T^{(2)}, \ldots, T^{(\beta)}$, a color weight can be expressed as

$$W_G = \sum_{r=1}^{\beta} w_{Gr} T^{(r)}, \tag{2.5}$$

where the coefficients w_{Gr} depend on the choice of the basis, but do not depend on the choice of the color group, i.e. they would be the same if the color group were E_7 instead of SU(3). In the Compton scattering example we took $T^{(1)} = W_a$, $T^{(2)} = W_b$, in which case the Lie algebra relation expresses W_c in this color basis as

$$W_c = (+1)T^{(1)} + (-1)T^{(2)}. \tag{2.6}$$

A color basis is not unique; any set of independent linear combinations of elements of a basis can equally well be used as a basis. On the other hand, the number of elements of the basis is fixed.

In this paper we give an algorithm for constructing color bases. In this algorithm one starts by writing down the color weights of all diagrams contributing in a given order in the perturbation expansion. Next one unravels all 3-gluon color vertices by means of the Lie algebra relation, fig. 3b. The remaining color weight diagrams look like QED Feynman diagrams. Finally one eliminates dependent color weights by a systematic application of the invariance relation fig. 3c. The color weights which can remain after all such relations have been exhausted form a color basis. We assert that the color basis obtained in this way is a maximal color basis. The reason is simple; for an arbitrary color group, the only tool we have available to relate color weights are the Lie algebra relations, and we have exhausted all of those.

3. Gauge sets

While the Green functions are gauge dependent, physical quantities like the S-matrix, the Wilson loop or the bound-state poles are gauge independent. In

perturbation theory the gauge invariance is implemented by Ward–Takahashi identities [9–11]. They guarantee that if $A = \sum_G A_G$ is the sum of all diagrams contributing to a given Green function in a given order in perturbation theory, then A gives a gauge-invariant contribution to the S-matrix. But if the gauge variation of A gives a vanishing contribution, and if A can be written as a sum of contributions to linearly independent color basis elements

$$A = \sum_{r=1}^{\beta} A_r T^{(r)}, \tag{3.1}$$

then each coefficient A_r separately gives a gauge-invariant contribution to the physical quantity in question. Such a sum of momentum integrals weighted by the color basis coefficients [defined by (2.5)]

$$A_r = \sum_G w_{Gr} C_G F_G \tag{3.2}$$

will be referred to as a *gauge set*. There are two important observations to be made about gauge sets. First, a gauge set is a gauge set for any gauge theory because (as shown in sect. 2) the coefficients w_{Gr} do not depend upon the choice of the group. For a particular gauge group, such as SU(3) or G_2, the color basis elements $T^{(r)}$ are not necessarily independent, but the gauge sets still give separately gauge-invariant contributions. The second observation is that a gauge set has no direct physical meaning, as the choice of the color basis is *a priori* arbitrary. However, a particular color basis choice might be dictated by a physical criterion, such as the leading log dominance of a certain class of diagrams.

We do not include any explicit checks of gauge invariance in this paper, as Ward identities are standard textbook material [10]. The reader is urged to check the gauge-invariance of a few simple gauge sets; for QED this amounts to the repeated applications of a single trivial identity [8].

$$\frac{1}{\not{p}+\not{K}-m} \not{K} \frac{1}{\not{p}-m} = \frac{1}{\not{p}-m} - \frac{1}{\not{p}+\not{K}-m}. \tag{3.3}$$

For QCD one also needs the corresponding identities for the gluon and ghost vertices [17–19].

4. Tree diagrams

In this section we construct a color basis for the tree diagrams consisting of one quark line and m external gluons. For $m = 3$ all such diagrams are drawn in fig. 4. Following our general procedure, we start by eliminating the color weights of the diagrams with 3-gluon vertices, figs. 4 g–p, by means of the Lie algebra relation fig. 3b. An example is given in fig. 5. As noted in sect. 2, the color weight of the four-gluon vertex diagram fig. 4p is a linear combination of the weights figs. 4m,n,o.
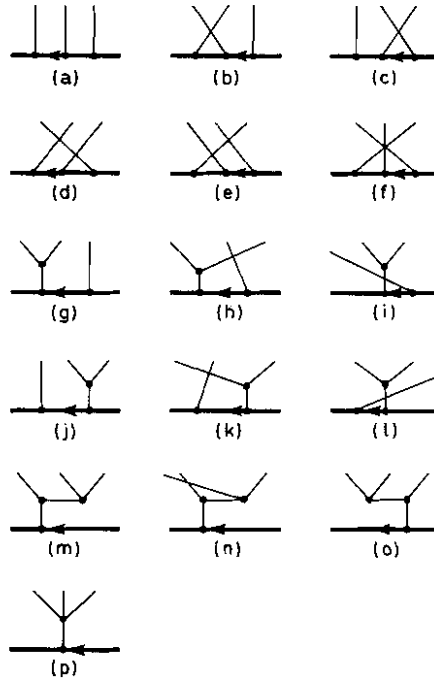
Fig. 4. Tree diagrams with three gluons, $m = 3$.

Six color weights remain, figs. 4a–f. They cannot be related by the Lie algebra relations and are therefore elements of the color basis. They are simply the 3! ways of multiplying the group generator matrices T_i, T_j and T_k. By the same reasoning, there are $m!$ gauge sets for trees with m external gluons.

The color basis we have just described corresponds to the $m!$ permutations of the external gluons. As no permutation is preferred, the corresponding gauge sets are democratic, in the sense that each of them receives contributions from the same number of diagrams. It is possible, however, to choose a different color basis which is of greater physical interest. Consider again the Compton scattering, fig. 2. If we choose the color basis $T^{(1)} = \frac{1}{2}(W_a + W_b)$, $T^{(2)} = \frac{1}{2}(W_a - W_b)$, the gauge sets are $A_1 = F_a + F_b$, $A_2 = F_a - F_b + 2F_c$. The symmetric set A_1 is the QED Compton scattering, while A_2 is the purely non-abelian contribution to Compton scattering.

In general one can construct a color basis for m gluons using the irreducible representations of S_m, the symmetric group of degree m. We work out the $m = 3$

Fig. 5. Example of the elimination of a 3-gluon vertex in a color weight diagram.
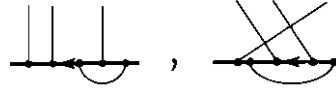
Fig. 6. Two examples of one-loop diagrams ($m = 3$).

example in appendix B. There is always one fully symmetric basis element which singles out the QED gauge set, while the remaining basis elements are non-abelian.

5. Adding loops

Let us now add one internal gluon to the tree diagrams just considered. By our first rule, we know that all 3-gluon color vertices can be immediately eliminated, so we only have to consider QED-like color weight diagrams, as in fig. 6. Next we use the invariance relation fig. 3c to move the left vertex of the internal gluon to the leftmost end of the quark line. An example of this procedure is given in fig. 7. Once this is done, all the invariance relations have been exhausted. Hence for m external gluons and $l = 1$ gluon loops there are $(m + 1)!$ independent color basis elements. An example is the color basis for 1-loop corrections to Compton scattering, fig. 8.

For the diagrams with m external gluons and $l = 2$ gluon loops we proceed as in the $l = 1$ case and reduce the color weights to $(m + 2)!$ weights with the two internal gluons originating from the left end of the quark line. This exhausts all invariance relations involving external gluons. However, this is not the end of the story; now we also have to take into account relations between internal gluons. A relation exists every time internal gluons are adjacent to each other, e.g. fig. 9a. We use it to remove $m(m!)$ "crossed rainbows" spanning external gluons. Further color weights are eliminated by relation fig. 9b. For example, the 2-gluon loop corrections to the quark form factor, $m = 1$, split up into 4 gauge sets corresponding to the color basis fig. 10.
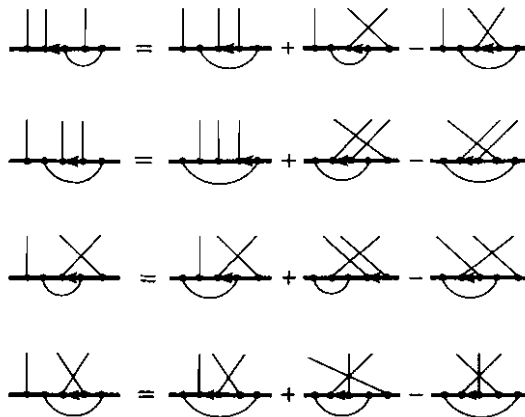

Fig. 7. Example of how the left end of an internal gluon is moved step by step to the left end of the fermion line.
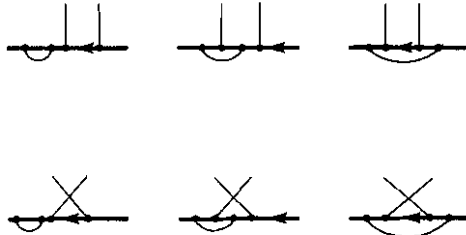
Fig. 8. Color basis for the 1-loop corrections to QCD Compton scattering.
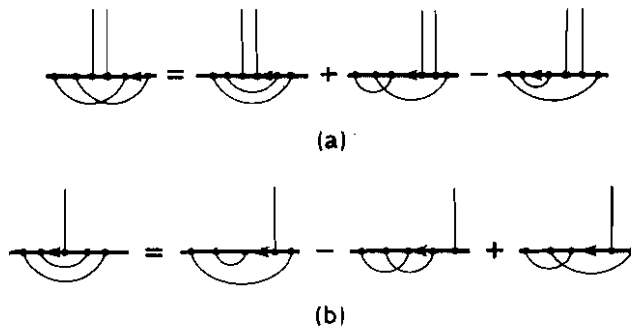
(a)

(b)

Fig. 9. (a) Unwinding of a "crossed rainbow". (b) A further relation.

One can proceed in this fashion for $l = 3, 4, \ldots$ loops, but we hope that our point has been made; it is always possible systematically to exhaust the Lie algebra relations to construct a color basis. We now leave the $q\bar{q} \rightarrow$ gluons processes in order to turn to the physically more interesting color singlet interactions.

For reasons of simplicity we omit three classes of QCD diagrams in this paper, which could easily be included. The first group are those diagrams with additional quark loops e.g. fig. 1d. As in QED, they form separate gauge sets because different quarks may have different masses. The second group are the color weights for pure gluon diagrams. They can be related directly to the single quark diagrams by
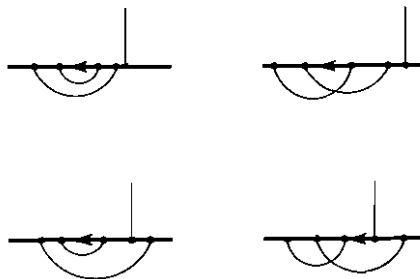
Fig. 10. Color basis for the 2-gluon-loop corrections to the quark form factor.
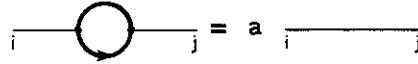
Fig. 11. Normalization of a fermion–loop insertion.

replacing one of the gluon propagators δ_{ij} in the pure gluon color weight diagram by $(1/a) \mathrm{Tr}\, (T_i T_j)$ (here a is a normalization factor). Diagrammatically this is represented by fig. 11. Finally, as we assume no particular gauge group, invariant color tensors such as ε_{abc} in the case of SU(3) are not included in our analysis. In other words, we do not consider baryons; when included, they will yield gauge sets over and beyond those obtained here.

6. Vacuum bubbles

If QCD is the correct theory of strong interactions, it is a theory of bound color singlet states. Bound-state kernels, meson decays and meson scatterings will involve diagrams like those in fig. 12a. At this time we still have no clue as to how such diagrams are to be evaluated and summed. The color weights for these diagrams, on the other hand, are easy to study. Diagrammatically these color weights have no external legs, as hadrons are color singlets; they are color vacuum bubbles. For example, the color weight for the meson–meson scattering diagram fig. 12a is given by fig. 12b. We shall now show how to use the color weights to split up contributions to such processes into gauge-invariant sectors.

We have already begun the construction of the color bases for vacuum bubbles in the previous section; we have only to take the trace of the color basis elements for the
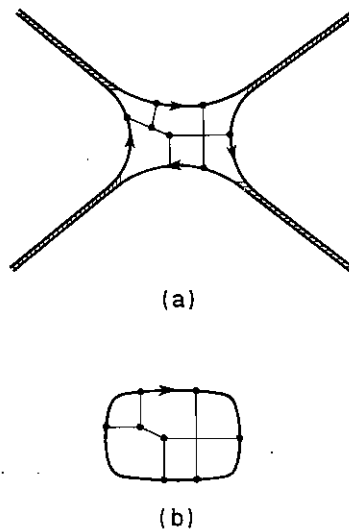

(a)

(b)

Fig. 12. (a) A typical meson–meson scattering diagram in QCD. (b) Color weight diagram for (a).
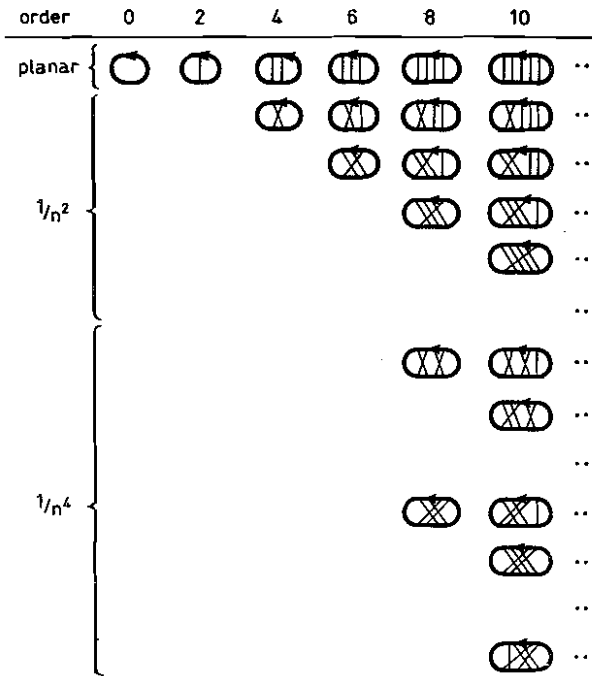
Fig. 13. Color basis for vacuum bubbles with one quark loop.

quark self-energy diagrams, i.e. the diagrams of the previous section without external gluons ($m = 0$). The color bases for the vacuum bubbles and the quark self-energy diagrams are equivalent (for a proof, see appendix A). To illustrate the classification that emerges, we have constructed the color bases up to order g^{12}. The results are tabulated in fig. 13 in a way which should be suggestive of the structure of the color bases to any order.

In order to illustrate the significance of these color bases, it is useful to make the comparison with the $U(N), N \to \infty$ analysis [12–15]. The top row of fig. 13 consists of color weights of the form $NC_2(R)^l$, where l is the number of gluon lines and $C_2(R)$ is the quadratic Casimir operator for the quark representation. The color weights of the

TABLE 1

Comparison of the number of the quark self-energy gauge sets and the number of QED-like quark self-energy diagrams (without fermion loop insertions)

Order	2	4	6	8	10	12	...	$2l$
Gauge sets	1	2	3	6	10	20	...	$\binom{l}{l/2}$
Feynman graphs	1	3	15	105	945	10 395	...	$(2l-1)!!$

The corresponding color bases are given in fig. 13. The general form $\binom{l}{l/2}$ is conjectured.

top row get contributions from all the planar QCD diagrams and only from these planar diagrams. This is also the set of diagrams selected by the $N \to \infty$ limit. Actually the planar gauge set is the $U(\infty)$ theory, up to a rescaling of the coupling constant by $C_2(R)$ factors. The difference between the two approaches is that the planar color weight defines the planar sector for any gauge theory.

Fig. 13 contains more information than can be obtained from the $N \to \infty$ limit. The first non-planar gauge set consists of diagrams with two neighboring gluon lines crossed. For a simple color group, these have color weights of the form $NC_v(R)C_2(R)^{l-1}$ where $C_v(R)$ is the vertex Casimir operator: $T_iT_jT_i = C_v(R)T_j$. $C_v(R)$ is linearly independent of $C_2(R)$; in $SU(N)$ for example, $C_v(R) = -1/N$, while $C_2(R) = (N^2-1)/N$.

The $U(N)$ topological counting rule, in contrast, combines these diagrams with those in which one gluon crosses more than just one neighboring gluon into a single next-to-leading non-planar correction. In general we find that each non-leading $U(N)$ correction is resolved into several gauge sets.

The usual interpretation of the $U(N)$ analysis is that it is a formal expansion in the "small parameter" $1/N$. Now the question arises how we should order our gauge sets. Group-theoretical considerations alone give no obvious small parameter like $1/N$. In fig. 13 we have ordered them by powers of various Casimir operators. We shall appeal to experience with QED bound states to argue that the dynamics of QCD may provide a natural ordering of gauge sets. In QED a lowest order approximation to the bound-state spectrum is obtained by summing the infrared logarithms of a gauge invariant subset of diagrams – the set of all cross-ladder exchanges [20]. It is possible that a lowest order approximation to the QCD bound state can be similarly obtained by isolating and summing the leading infrared divergences. According to the infrared power-counting theorems [21, 22], the leading infrared divergences may occur in both the planar and non-planar gauge sets in the basis of fig. 13. A more detailed analysis of the infrared structure of perturbative QCD is required to determine a color basis in which the gauge sets are ordered according to how strongly they contribute to the binding.

A realisation of the above ideas is two-dimensional QCD in axial gauge. In this model, the leading infrared singularities are contained in the planar gauge set, with the non-planar sectors suppressed by powers of the infrared cutoff [22].

Gauge sets could also play an important role in controlling the convergence of QCD. Because of the slow growth [23–25] of the number of diagrams with the order k, the planar perturbation series will converge for a sufficiently small coupling if the numerical value of the individual diagrams is bounded [24]. In a gauge theory the value of an individual Feynman graph is gauge dependent; only the value of a gauge-invariant set of such diagrams is meaningful. As gauge sets are often characterized by large cancellations between contributing diagrams [2], it is possible that the contribution of a gauge set may grow much more slowly than the total number of diagrams [26]. In that case it is interesting to observe that the number of gauge sets
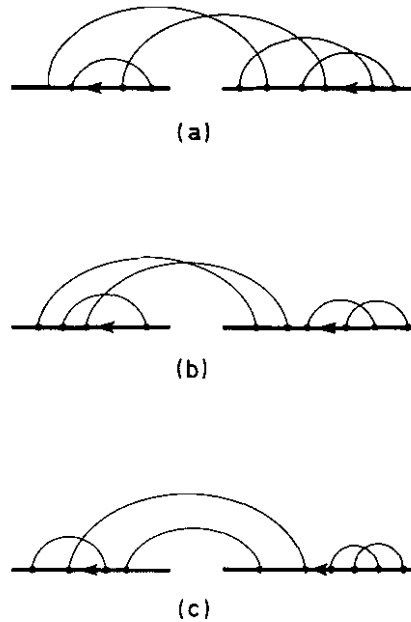
(a)

(b)

(c)

Fig. 14. Examples of color weight diagrams for quark–quark scattering.

increases slowly with order. The number of gauge sets in fig. 13 is, by extrapolation, $\binom{l}{l/2}$ in $2l$th order, and thus grows as the lth power of a constant. One can then hope that the non-planar gauge sets do not spoil the conjectured convergence of the planar perturbation expansion.

7. Quark–quark scattering

As our last example we discuss gauge sets for quark–quark scattering. These are physically interesting as they can be used as kernels for the meson bound-state equations. They are also used in the study of QCD infrared divergences. We limit ourselves to connected quark–quark scattering graphs without internal quark loops.

The procedure is simple and consists of three steps. The first one is the elimination of all 3-gluon vertices by the Lie algebra relation fig. 3b. The remaining color weights are represented by QED-like diagrams; a typical one is drawn in fig. 14a. Now one moves those gluons, both ends of which are attached to the right fermion line, to the rightmost end of that line by repeated application of the Lie algebra relation, fig. 3c. The resulting diagrams then have the following structure: a number of self-energy insertions on the right fermion, a number of (possibly crossed) gluons connecting the fermions, and all possible self-energy insertions on the left fermion. A typical example is fig. 14b. Now, the crossed rainbows can be unwound and insertions on the left fermion line ordered as in sect. 5 by means of the Lie algebra relation fig. 3c. The
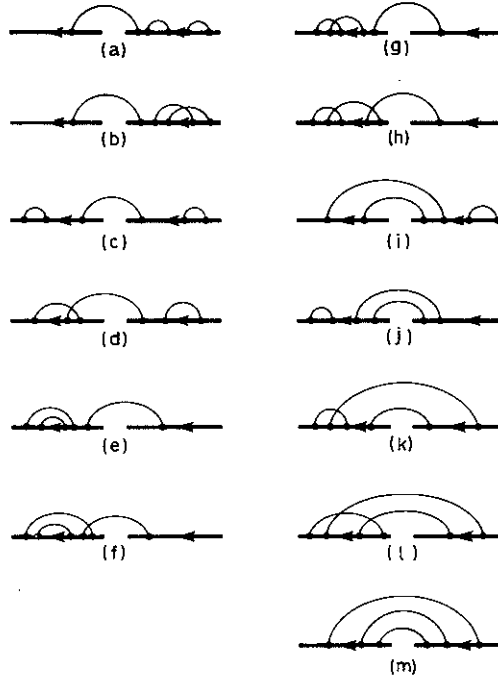
Fig. 15. Color basis for quark–quark scattering in sixth order.

diagrams obtained in this way are of the type of fig. 14c. The conclusion is that the quark–quark scattering color basis follows trivially from the color basis constructed in sect. 5. As an example we show in fig. 15 the color basis for quark–quark scattering in sixth order. There are 13 gauge sets in this case. An interesting observation about this choice of color basis is that some of the gauge sets receive contributions from very few Feynman diagrams. For example, the gauge set corresponding to the color weight fig. 15m gets contributions only from the six 3-gluon exchange diagrams; in other words, this set isolates the QED crossed ladders gauge set. If one wished to focus upon the non-abelian features of the theory, a convenient small gauge set would be fig. 15l, which only gets contributions from the 14 diagrams drawn in fig. 16.

An example of the utility of the color bases is provided by the calculation of QCD non-leading IR divergences of ref. [27, 28]. Consider for example quark–quark scattering in order g^4, fig. 1. The corresponding color basis obtained by our algorithm is given by fig. 17a. Instead of the basis element (iii), we can use the quadratic Casimir operator for the adjoint representation, related to (iii) by fig. 17b. For a simple Lie group this basis element can be written as $C_2(G)(T_i)_b^a (T_i)_d^c$. The corresponding non-abelian gauge set ($C_2(G) = 0$ for an abelian theory) is given in fig. 17c. The IR divergences occurring in the analogous non-abelian gauge sets for the process $q + q \rightarrow q + q + \gamma^* + 2$ soft gluons were investigated by the authors of [27].
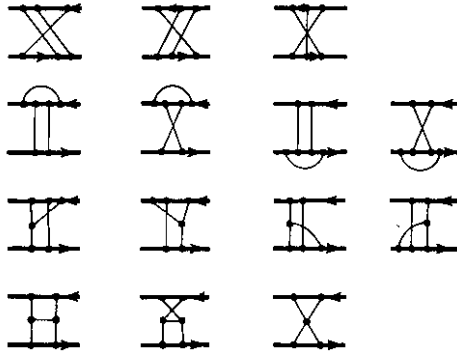
Fig. 16. Feynman diagrams contributing to the gauge set corresponding to color weight (1) in fig. 15.

8. QED gauge sets

In the introduction we gave an example of a gauge set in QED and went on to consider the problem of how to find gauge sets in arbitrary non-abelian gauge theories. Our solution relies on the Lie algebra structure of the color weights, and one may ask what relation the QCD gauge sets have to the more familiar QED gauge sets.
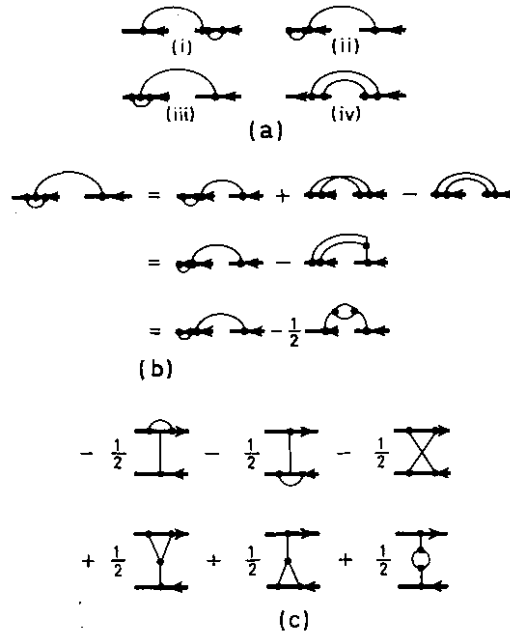

Fig. 17. (a) Color basis for quark–quark scattering in order g^4. (b) The relation of color basis element (iii) to the quadratic Casimir basis element. (c) Gauge set corresponding to the color basis element $C_2(G)(T_i)_b^a(T_i)_d^c$. Color basis coefficients w_G, from (3.2) are given explicitly; diagrams stand for the remaining factors $C_G F_G$. Ghost and seagull gluon self-energy diagrams are not drawn.
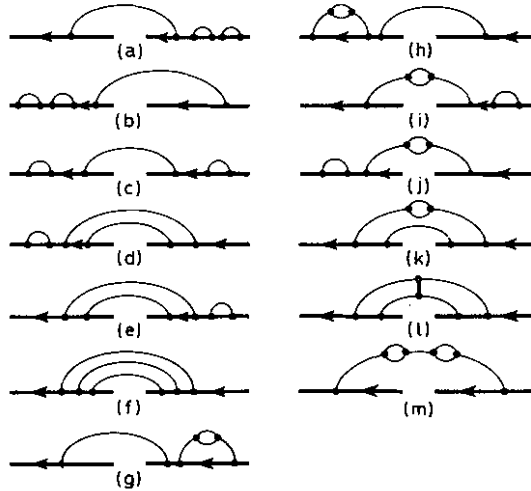
Fig. 18. An alternative choice of color basis for quark–quark scattering in sixth order. Gauge sets corresponding to (a)–(f) consist of QED-like Feynman diagrams only.

In our construction of color bases a considerable simplification was achieved by the elimination of all color weights with 3-gluon color vertices. If one wishes to display the QED gauge sets explicitly, it is more convenient to choose a color basis in which a maximum number of basis elements have explicit 3-gluon color vertices. Such basis elements vanish for an abelian group, and the remaining basis elements correspond to the usual QED gauge sets.

For example, the color basis for quark–quark scattering in order g^6, fig. 15, can be replaced by the color basis of fig. 18. Diagrams (a) to (f) correspond to the six QED gauge sets of electron–muon scattering in order e^6 (diagrams with fermion loops contribute to further gauge sets).

9. Conclusions

In this paper we have shown how the color structure of an arbitrary non-abelian gauge theory can be used to decompose the perturbation expansion into gauge-invariant sectors. The resulting classification applies to any gauge theory. We believe it to be the maximal resolution into gauge-invariant sectors, in the sense that there should be no gauge set that cannot be written as a linear superposition of our gauge sets.

We have argued that the gauge sets should be useful in organising QCD bound-state calculations. If a particular gauge set can be established as a zeroth-order approximation to the bound-state wave function, the remaining gauge set decomposition will give the systematics of the non-leading corrections.

Gauge sets also have immediate practical applications. They provide independent checks on higher order perturbative calculations by defining various gauge-invariant

combinations of contributions. This also makes it possible to compare intermediate results calculated in different gauges.

Gauge sets provide a gauge-invariant way of isolating the purely non-abelian effects in gauge theories, such as the non-cancellation of the non-leading IR divergences [27].

Appendix A

RELATIONS BETWEEN COLOR WEIGHTS

The color weight diagrams are in mathematical language invariant tensors of the gauge group. This means that if we perform a gauge group transformation of the color coordinate system, the expression for these tensors in the new coordinate system is identical to the expression in the old system. Perhaps the simplest example is the three-gluon vertex $-iC_{ijk}$. After an infinitesimal gauge transformation, we have

$$C'_{ijk} = C_{ijk} + \varepsilon_l \{ C_{lii'} C_{i'jk} + C_{ljj'} C_{ij'k} + C_{lkk'} C_{ijk'} \} + O(\varepsilon^2) \,. \tag{A.1}$$

The term in brackets vanishes by the Jacobi relation. Using the notation of fig. 3, the Jacobi relation is given in fig. 19a. Hence the structure constants are invariant tensors. Similarly, after an infinitesimal gauge group transformation, the quark–antiquark–gluon vertex is given by

$$(T'_i)^a_b = (T_i)^a_b + i\varepsilon_l \{ -iC_{lii'} (T_{i'})^a_b + (T_l)^a_{a'} (T_i)^{a'}_b - (T_l)^{b'}_b (T_i)^a_{b'} \} \,. \tag{A.2}$$

Again the term in the brackets vanishes by the Lie algebra

$$[T_l, T_i] = iC_{lii'} T_{i'} \,, \tag{A.3}$$

and the generators $(T_i)^b_a$ are invariant tensors. Furthermore, any combination of invariant tensors, with or without contracted indices, is itself an invariant tensor. In particular, all color weights of gauge theory Feynman diagrams are invariant tensors.

As a consequence of the Lie algebra every color weight satisfies an *invariance relation* analogous to the basic relations fig. 3b and fig. 19a. As an example, consider a color weight W^{ab}_{cdi} for a diagram with two external quarks, two external antiquarks and one external gluon. The reader can check by repeated use of Lie algebra on any color weight diagram of this type that

$$W^{a'b}_{cdj} (T_k)^a_{a'} + W^{ab'}_{cdj} (T_k)^b_{b'} - W^{ab}_{c'dj} (T_k)^{c'}_c - W^{ab}_{cd'j} (T_k)^{d'}_d + W^{ab}_{cdi'} (-i) C_{kj'j} = 0 \,. \tag{A.4}$$

Diagrammatically the above relation is given by fig. 19b.
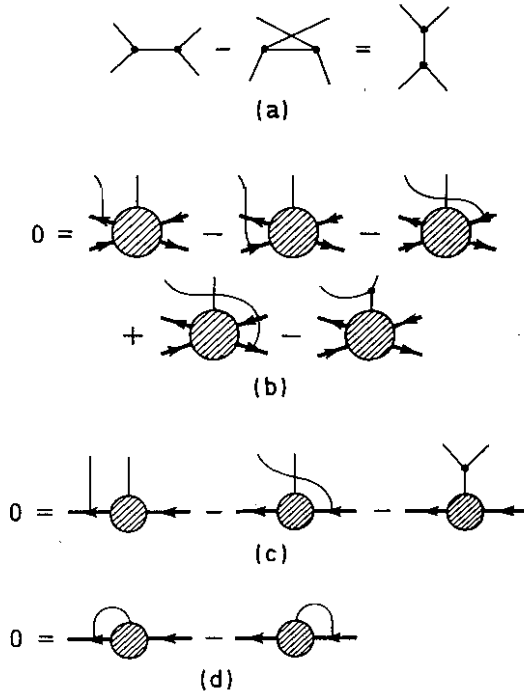
Fig. 19. (a) Jacobi identity. (b) Example of an invariance relation. (c) Invariance relation for quark form-factor. (d) Equality of self-energy color weights.
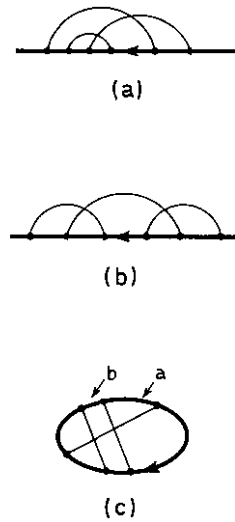

Fig. 20. Quark self-energy color weights (a), (b) obtained by cutting the vacuum bubble (c) in two ways.

The diagrammatic representation of invariance relations is useful in relating whole classes of color weights. A simple example is the invariance relation for color weight diagrams contributing to the quark form factor, fig. 19c. Contracting the two gluon color indices and using the antisymmetry of C_{ijk} we obtain the relation fig. 19d. In the beginning of sect. 6 we asserted that the color bases for quark self-energies and vacuum bubbles are equivalent. This is perhaps most easily seen by taking a vacuum color bubble diagram and cutting the quark line in all possible ways. Cutting to the left and to the right of a given gluon vertex, one obtains two different self-energy color weights, as in fig. 20. However, by the relation fig. 19d, these color weights are equal. Further such relations are an important tool in constructing higher order color bases, such as in fig. 13.

(a)

(b)

(c)

(d)

(e)

Fig. 21. (a) Symmetrization operation for three lines. For m lines it is the sum of all $m!$ permutations. (b) The antisymmetrization operation is the alternating sum of $m!$ permutations. (c) Decomposition of the identity permutation into a fully antisymmetric, a fully symmetric and two mixed symmetry representations. Corresponding Young tableaux are given. (d) Decomposition of a permutation in terms of an orthonormal basis. (e) Permutation (23) expanded in this basis.

Appendix B

SYMMETRIC GROUP AND COLOR BASES

In sect. 4 we have noted that in the case of Compton scattering, the choice of a symmetrized color basis separates the QED-like sector from the purely non-abelian sector. In this appendix we shall show how the symmetric group can be applied to the construction of a $q\bar{q} \rightarrow (m$ gluons) color basis. As there already exists an extensive literature on the symmetric group [29], we shall restrict ourselves to establishing contact with the literature by discussing the first non-trivial example, the three gluon case, $m = 3$.

According to sect. 4, there are 3! elements in the color basis for the diagrams of fig. 4, which we wish to rewrite in terms of symmetric and antisymmetric combinations. In order to do this, we introduce a symmetrization operator, fig. 21a, denoted by a white bar, and an antisymmetrization operator, fig. 21b, denoted by a black bar. We decompose the identity into four orthonormal projection operators, as in fig. 21c. The choice of the last two projectors is arbitrary; the reader can check the identity by expanding all symmetrizations and antisymmetrizations. In this way we obtain 4 symmetric color basis elements; the remaining 2 are obtained by sandwiching permutations (other than the identity) between the mixed symmetry projection operators. An arbitrary permutation $W_{\mathrm{G}} = \sigma$ can now be expanded as a linear combination of the elements of this basis:

$$W_{\mathrm{G}} = W_{\mathrm{G,A}} T^{(A)} + W_{\mathrm{G,S}} T^{(S)} + W_{\mathrm{G,11}} T^{(11)} + W_{\mathrm{G,12}} T^{(12)} + W_{\mathrm{G,21}} T^{(21)} + W_{\mathrm{G,22}} T^{(22)} .$$

(B.1)

Fig. 21d is the diagrammatical representation of this expansion and in fig. 21e we give as an example the expansion for a specific permutation (23). The factors for the

(a)

(b)

Fig. 22. (a) The fully antisymmetric gauge set, with the coefficients σ_{A} from fig. 20d explicitly displayed. (b) The gauge set corresponding to the σ_{11} color basis element in fig. 20d.

off-diagonal basis elements are adjusted so that this is precisely the orthonormal basis

$$\begin{pmatrix} \sigma_{11} & \sigma_{12} \\ \sigma_{21} & \sigma_{22} \end{pmatrix} = \begin{pmatrix} -\frac{1}{2} & \frac{1}{2}\sqrt{3} \\ \frac{1}{2}\sqrt{3} & \frac{1}{2} \end{pmatrix} \tag{B.2}$$

of table 7–3 of ref. [29]. The interested reader can also consult [30] for an explicit $m = 4$ symmetric group basis.

The $m = 3$ non-abelian tree diagrams may now be assembled into six gauge sets corresponding to the six projectors $T^{(p)}$ with weights given by the coefficients W. The four-gluon vertex color weight can be expressed as a sum of three-gluon vertex color weights and every three-gluon vertex color weight can be rewritten in terms of QED-like diagrams which are permutations of the identity.

Unlike the color basis of sect. 4, symmetric group color bases extract gauge sets with different numbers of diagrams. The gauge set corresponding to the fully symmetric Young tableau is always the QED gauge set: the sum of $m!$ QED-like diagrams, figs. 4a–f. The gauge set corresponding to the fully antisymmetric Young tableau is given in fig. 22a. Diagrams 4m–p do not contribute because of the Jacobi identity. A typical mixed symmetry gauge set, corresponding to the σ_{11} coefficients in fig. 21d, is given in fig. 22b. (We have not displayed the contributions from the four-gluon vertex diagram in order to avoid introducing more diagrammatic notation [19], but such extension is straightforward.)

References

[1] B.E. Lautrup, A. Peterman and E. de Rafael, Phys. Reports 3 (1972) 4
[2] P. Cvitanović, Nucl. Phys. B127 (1977) 176
[3] G. Feldman, T. Fulton and D.L. Heckathorn, Nucl. Phys. B174 (1980) 89
[4] D.R. Yennie, S.C. Frautschi and H. Suura, Ann. of Phys. 13 (1961) 379
[5] S. Weinberg, Phys. Rev. 140 (1965) B516
[6] G. Grammer and D.R. Yennie, Phys. Rev. D8 (1973) 4332
[7] C.P. Korthals Altes and E. de Rafel, Nucl. Phys. B106 (1976) 237;
    J.S. Ball, D. Horn and F. Zachariasen, Nucl. Phys. B132 (1978) 509
[8] J.D. Bjorken and S.D. Drell, Relativistic quantum fields (McGraw-Hill, New York, 1965).
[9] G. 't Hooft, Nucl. Phys. B33 (1971) 173
[10] W. Marciano and H. Pagels, Phys. Reports 36 (1978) 137
[11] B.W. Lee, *in* Methods in field theory, ed. R. Balian and J. Zinn-Justin, Les Houches, Session XXVIII, 1975 (North-Holland, Amsterdam, 1976)
[12] G. 't Hooft, Nucl. Phys. B72 (1974) 461
[13] G. 't Hooft, Nucl. Phys. B75 (1974) 461
[14] E. Witten, Nucl. Phys. B160 (1979) 57
[15] S. Coleman, 1979 Erice Lectures, SLAC preprint PUB-2484 (March, 1980)
[16] P. Cvitanović, Phys. Rev. D14 (1976) 1536
[17] G. 't Hooft, Nucl. Phys. B33 (1971) 173
[18] B. Lautrup, Of ghoulies and ghosties, Niels Bohr Inst. preprint NBI-HE-76-14 (Aug., 1976)
[19] P. Cvitanović, Nucl. Phys. B130 (1977) 114
[20] E. Brézin, C. Itzykson and J. Zinn-Justin, Phys. Rev. D1 (1970) 2349;
    M. Lévy and J. Sucher, Phys. Rev. 186 (1969) 1656

[21] P. Cvitanović and T. Kinoshita, Phys. Rev. D10 (1974) 3991;
     T. Kinoshita and A. Ukawa, Phys. Rev. D15 (1977) 1596; D16 (1977) 332
[22] J.M. Cornwall and G. Tiktopoulos, Phys. Rev. D15 (1977) 2937
[23] W.T. Tutte, Can. J. Math. 14 (1962) 21
[24] J. Koplik, A. Neveu and S. Nussinov, Nucl. Phys. B123 (1977) 109
[25] E. Brézin, C. Itzykson, G. Parisi and J.B. Zuber, Comm. Math. Phys. 59 (1978) 35
[26] C.A. Hurst, Proc. Roy. Soc. A214 (1952) 44;
     P. Cvitanović, B. Lautrup and R.B. Pearson, Phys. Rev. D18 (1978) 1939
[27] R. Doria, J. Frenkel and J.C. Taylor, Nucl. Phys. B168 (1980) 93
[28] C. Di'Lieto, S. Gendron, I.G. Halliday and C.T. Sachrajda, Nucl. Phys. B183 (1981) 223
[29] M. Hamermesh, Group theory and its application to physical problems (Addison-Wesley, Reading,
     Mass., 1962)
[30] P. Cvitanović, R.J. Gonsalves and D.E. Neville, Phys. Rev. D18 (1978) 3881